Preliminary Simulation Results of a Deeply Coupled GPS/INS System for High Dynamics

Stefan Kiesel, Andreas Maier, Ulrich Seiller, Gert F. Trommer
Karlsruhe Institute of Technology, KIT

BIOGRAPHY

Stefan Kiesel is a Dr.-Ing. (Ph.D.) candidate at the Institute of Theory and Systems Optimization in Electrical Engineering of the Karlsruhe Institute of Technology (KIT), Germany. He received his Diploma (M.S.) in Electrical Engineering in 2006 from the University of Karlsruhe. His areas of research include strapdown inertial navigation systems, GPS/INS integration, and software GPS receivers.

Andreas Maier is a Dr.-Ing. (Ph.D.) candidate at the Institute of Theory and Systems Optimization in Electrical Engineering of the Karlsruhe Institute of Technology (KIT), Germany. He received his Diploma (M.S.) in Electrical Engineering in 2005 from the University of Karlsruhe. His areas of research include SAR/INS integration and federated Kalman filter design for data fusion.

Ulrich Seiller received his Diploma in Electrical Engineering of the University of Karlsruhe in 2009. He was involved in GPS/INS research projects.

Gert F. Trommer received the Dipl.-Ing. (M.S.E.E.) and the Dr.-Ing. (Ph.D.) degrees from the TU Munich, Germany in 1978 and 1982, respectively.
He joined EADS/LFK, formerly MBB/Dasa, where he was project manager for the IMU development in the UK ASRAAM program. He was director of the section "Flight Control Systems" with the responsibility for the Navigation, Guidance and Control Subsystem, the IR Seeker and the Fin Actuators in the German/Swedish Taurus KEPD 350 program. Since 1999 he is director of the "Institute of Systems Optimization" at the Karlsruhe Institute of Technology, with research focus on INS/GPS/TRN integrated navigation systems and UAVs. Since 2004 he is dean of the "Department of Electrical Engineering and Information Technology".

ABSTRACT

Deeply coupled GPS/INS integration combines GPS signal tracking and the navigation problem into one processing step. Dynamic information from an inertial measurement unit (IMU) is used to compensate trajectory dynamics in the signal tracking process. This offers new possibilities in designing the GPS baseband processor. Non-coherent deep integration uses discriminator information as direct or smoothed measurement of the residual tracking error. This measured tracking error used in the Kalman filter measurement step is basically a measurement averaged over the predetection integration time. Discriminator values resulting from correlator outputs in general describe an average tracking error.

For increasing the predetection integration time a systematically correct description of the measurement is necessary. In existing deeply coupled GPS/INS systems these averaged measurements are used as punctual values which produces systematic errors especially visible in high dynamics.

The proposed deeply coupled GPS/INS integration system uses these averaged values in an adequate measurement step. By imitating the approach of time differenced carrier phase measurements, a measurement formulation was found that accounts for the systematic inconsistency. In this formulation trajectory dynamics are modelled in the measurement step. The accuracy of the navigation process in high-acceleration environments up to 35g is significantly increased and the velocity error in the simulation is lower than 5cm/s.

1. INTRODUCTION

Current research is conducted on the field of Kalman filter based signal tracking that includes inertial sensors. The navigation process and the signal tracking process are performed simultaneously which is also called deeply coupled GPS/INS integration. The signal tracking process is supported by trajectory dynamics measured by an inertial navigation system. This enables new possibilities in designing the base band processor including GPS/INS integration.

In a tightly coupled GPS/INS integration system measurements of standard GPS signal tracking loops are used as measurement in the navigation filter. These measurements are not filtered by a Kalman filter inside the GPS receiver. The resulting position and velocity estimation can be used as aiding information for standard signal tracking loops. The basic structure of the loop design remains untouched and an estimated relative LOS velocity is used to compensate for the dynamics. As a result the bandwidth of the loop filter can be reduced or adapted dynamically depending on the noise environment [5]. A low bandwidth results in a long time interval between uncorrelated measurements. However, time-correlated measurements can be a problem for a Kalman filter used for data fusion.

Deeply Coupled GPS/INS Integration solves the navigation and tracking problem by a central navigation filter instead. Measurement residuals and inertial data are used for calculating position and velocity updates that are used for controlling the signal correlation process. Single loop filters in standard tracking loops are replaced by a central navigation filter that controls the NCOs (numerically controlled oscillators). Using *I* and *Q* correlator outputs directly as measurements is commonly referred as coherent deep integration. The *Is* and *Qs* depend on the code phase error and the carrier phase error. For coherent deep integration the carrier phase has to be known in the Kalman filter. Pre-processing *Is* and *Qs* in discriminator functions avoids the necessity of the carrier phase information in the Kalman filter and uses only code phase errors and carrier frequency errors as measurements. This is known as non-coherent deep integration and is the optimal integration level for poor signal-to-noise and high dynamic environments.

In a common hardware software GPS receiver design $I_{E,P,L}$ and $Q_{E,P,L}$ (early, prompt and late) correlator outputs are provided every 1ms by each channel. For better noise performance these 1ms samples are integrated coherently over a predetection integration time (PIT). This predetection integration time can be up to 20ms without considering databit information and can be longer (reasonably up to 100ms) when using a databit estimation process [6]. Discriminator functions using these integrated *I* and *Q* samples output an average tracking error over the predetection integration time. Especially in high dynamic situation the averaging effect in the frequency error becomes apparent. Using an average Doppler frequency error with traditional range-rate (delta-range) measurement step produces systematic errors during high accelerations.

This paper studies the usage of a refined measurement formulation which was originally invented to process time-differenced accumulated delta range information [2, 3]. It uses the information of the transition matrix to correctly predict the difference in position in a specific time interval. This can be seen as a good estimation of the average relative velocity during the measurement interval. This measurement formulation can be adapted for processing averaged frequency error discriminator outputs.

In modernized GPS signal design and in upcoming Galileo signals, pilot signals with no navigation data bit modulation will be available for signal tracking. With these signals the predetection integration time can be easily extended over the 20ms databit time interval of the GPS C/A-code. But even with the existing GPS signal there are strategies for extending the predetection integration time by a data bit estimation process explained in [6]. This offers better noise performance but emphasizes the need for an adapted measurement step accounting for averaged measurement errors.

Although GPS/INS deep integration is developed for high anti-jamming environments, this capability is not shown here. This paper concentrates on the dynamic behavior. Nevertheless with the possibility of extended coherent pre-detection integration time, which can be used with navigation bit estimation or with modern GNSS pilot signals, this will also bring a benefit in anti-jamming behavior.

In [6] a deeply coupled GPS/INS system is presented that uses a *dynamics EKF* with transition matrix factorization together with GPS block processing. For block processing digital intermediate frequency samples (IF) must be available which results in a dramatically different hardware software setup of the receiver. When using traditionally available correlator hardware, these IF-samples are not available. Correlator samples with a rate of 1000 Hz or lower must be processed instead, which is done in the presented approach.

The remainder of the paper is structured as follows. Chapter 2 gives an overview of the system architecture. The applied signal tracking process is explained in general. Chapter 3 describes the measurement step extending time-differenced accumulated delta range measurement by the measurement of a frequency error. Chapter 4 details the potential of extended predetection integration time in a carrier frequency discriminator. Chapter 5 analyzes different update rates for the carrier frequency. Chapter 6 illustrates the simulation environment and chapter 7 shows simulation results.

2. SYSTEM ARCHITECTURE

A non-coherent deeply coupled GPS/INS system primarily processes outputs of discriminator functions converting $I_{E,P,L}$ and $Q_{E,P,L}$ to a code phase error and a carrier frequency error. The received correlator output can be modeled as [4]

$$\begin{aligned} I_E &= Ad_i\, R\left(x - d/2\right)\cos\left(\delta\phi_{ca}\right) + n_{IE} \\ I_P &= Ad_i\, R\left(x\right)\cos\left(\delta\phi_{ca}\right) + n_{IP} \\ I_L &= Ad_i\, R\left(x + d/2\right)\cos\left(\delta\phi_{ca}\right) + n_{IL} \end{aligned} \qquad (1)$$

$$
\begin{aligned}
Q_E &= Ad_i\, R(x - d/2)\sin(\delta\phi_{ca}) + n_{QE} \\
Q_P &= Ad_i\, R(x)\sin(\delta\phi_{ca}) + n_{QP} \\
Q_L &= Ad_i\, R(x + d/2)\sin(\delta\phi_{ca}) + n_{QL} \\
A &= \sqrt{2a(c/n_0)\tau_a}\,\mathrm{sinc}(\pi\delta f_{ca}\tau_a)
\end{aligned}
$$

Where A is the signal amplitude depending on the carrier-to-noise ratio c/n_0, and the average frequency error δf_{ca} in the integration interval of the correlator τ_a. The $I_{E,P,L}$ and $Q_{E,P,L}$ also depend on the code correlation function R, the databit d_i and the average phase error $\delta\phi_{ca}$. Since carrier frequency tracking is known to be more robust comparable to carrier phase tracking in high dynamic and in high jamming situations the $I_{E,P,L}$ and $Q_{E,P,L}$ are converted to code and frequency errors by discriminator functions. For code tracking a non-coherent code discriminator is employed that results in a code tracking error

$$
\tilde{D}_{Diskr} = \sqrt{I_E{}^2 + Q_E{}^2} - \sqrt{I_L{}^2 + Q_L{}^2}\,. \tag{2}
$$

The discriminator output has to be normalized by an estimation of the amplitude. In strong SNR situations $I^2 + Q^2$ is suitable while in poor SNR situations a c/n_0 has to be employed.

$$
\Delta\tilde{\rho}_{psr} = \tilde{D}_{Diskr}\frac{c_0}{f_{co}} \tag{3}
$$

transforms the discriminator output to a tracking error in meters. Although this tracking error could build the innovation for the Kalman filtering process, it is combined with the measured pseudorange of the replica signal $\tilde{\rho}_{psr}$. Thus position estimation refers to the same sampling time for each channel of a fundamental time frame given by the receiver hardware. Using the measured replica code phase for controlling the code NCOs is also done in [7], but in a different way.

As a navigation filter a closed loop error state space formulation of a Kalman filter is used with the states:

$\delta\vec{x}$	position errors (3)
$\delta\vec{v}^n_{eb}$	velocity errors (3)
$\delta\vec{\psi}$	attitude error (3)
$\delta\vec{a}^b_{ib}$	errors of estimated accelerometer biases (3)
$\delta\vec{\omega}^b_{ib}$	errors of estimated gyroscope biases (3)
$c\delta t$	error of receiver clock error (1)
$c\delta\dot{t}$	error of receiver clock error drift (1)

After the measurement step the strapdown is corrected and the state vector is set to zero.

The estimated position can be transformed to an estimated pseudorange $\hat{\rho}_{psr}$ including a position update induced by a tracking error. This estimated pseudorange can now be compared with the former pseudorange corresponding to the code phase of the replica signal $\tilde{\rho}_{psr}$. The error $\Delta\hat{\rho}_{psr}$ can be employed to control the code NCO towards minimizing the offset. This is also done because code phase steps are not possible in most GPS receivers. The NCO must be controlled by adjusting the code frequency. By aligning the replica code with the estimation of the navigation filter the discriminator only contains the tracking error. The observer (Kalman filter) and the controller (NCO controller) are realized separately.

The same is done with the frequency error received from a carrier frequency discriminator. A cross product formulation is employed that can either be normalized by the estimated carrier-to-noise ratio c/n_0 or can be used in a 4 quadrant arctan-function resulting in the carrier frequency tracking error $\Delta\tilde{f}_{ca}$.

$$
\begin{aligned}
cross &= I_{PS,1}\cdot Q_{PS,2} - I_{PS,2}\cdot Q_{PS,1} \\
dot &= I_{PS,1}\cdot I_{PS,2} + Q_{PS,1}\cdot Q_{PS,2} \\
\Delta\tilde{f}_{ca} &= \frac{1}{2\pi\cdot\frac{\Delta t}{2}}\arctan2(cross, dot)
\end{aligned} \tag{4}
$$

By applying the speed of light c_0 and the nominal carrier frequency f_{L1} a LOS velocity error can be calculated.

$$
\Delta\tilde{v}_{dop} = -\Delta\tilde{f}_{ca}\frac{c_0}{f_{L1}} \tag{5}
$$

In low dynamic situations the velocity error including the satellite velocity $\vec{v}^n_S$, lever arm $\vec{l}^{\,b}$, attitude estimation C^n_b, and angular rate $\vec{\omega}^b_{ib}$ might be the input for a velocity estimation process in the Kalman filter according to the measurement model

$$
\tilde{v} = \vec{e}^{\,T}\left(\vec{v}^n_S - \left(\vec{v}^n_U + C^n_b\vec{\omega}^b_{ib}\times\vec{l}^{\,b}\right)\right) + c_0\delta\dot{t} + n_v\,. \tag{6}
$$

The updated velocity estimation will be employed to calculate an estimated Doppler frequency that directly controls the carrier NCOs.

$$
\hat{f}_{ca} = f_{IF} - \frac{f_{L1}}{c_0}\hat{v}_{dop} \tag{7}
$$

In high dynamic environments with high accelerations and jerks this leads to a systematic error since $\Delta\tilde{f}_{ca}$ contains the average tracking error in the correlation time interval. This can lead to a misinterpretation and finally to inaccurate velocity estimations. To solve this problem, a method is applied that originally was developed to process time differenced accumulated delta ranges (ADR) and is now extended by an average frequency error.

3. REFINING THE MEASUREMENT STEP

One possibility of increasing velocity accuracy especially in high acceleration environments is to employ a measurement formulation that accounts for averaging effects during the time between measurements, meaning the correlator time interval described above. The derivation is similar to [2, 3]. Accumulated delta ranges can be described as

$$(\phi + N)\lambda = r_{SA} + c\delta t + \delta_{cm} + \delta_{mp} + n_{rcvr} \,. \qquad (8)$$

Building differences of two consecutive measurements leads to

$$(\phi_k - \phi_{k-1})\lambda = r_{SA,k} - r_{SA,k-1} + c\delta t_k - c\delta t_{k-1} + n'_k \qquad (9)$$

By using carrier phase time differences in an error state Kalman filter it has to be compared with the estimated change in position including the clock drift δt_k

$$\begin{aligned} \Delta y_k &= \hat{r}_{SA,k} - \hat{r}_{SA,k-1} + \Delta t \cdot c\delta\hat{t}_k - (\tilde{\phi}_k - \tilde{\phi}_{k-1})\lambda \\ &= \hat{y}_k - \tilde{y}_k \end{aligned} \qquad (10)$$

One way to find the appropriate measurement matrix $\mathbf{H}_k$ in the measurement formula in the measurement equation

$$\Delta\vec{y}_k = \mathbf{H}_k \Delta\vec{x}_k + \vec{v}_k \qquad (11)$$

is to apply a transition matrix factorization as follows:

$$\begin{aligned} \mathbf{H}_{\mathrm{k}} = \mathbf{H}_{\mathrm{k}}^{\#} \cdot \Big(& \vec{0}^T, \vec{0}^T, -\vec{\mathrm{e}}_{\mathrm{k}}^{\mathrm{T}} \left[\delta\hat{\vec{\mathrm{L}}}_{\mathrm{k}}^{\mathrm{n}} \times \right], \vec{0}^T, \\ & -\Delta\mathrm{t} \cdot \vec{\mathrm{e}}_{\mathrm{k}}^{\mathrm{T}} \left[\hat{\vec{\mathrm{L}}}_{\mathrm{k-1}}^{\mathrm{n}} \times \right] \hat{C}_{b,k}^{n}, 0, 0 \Big) \end{aligned} \qquad (12)$$

with

$$\mathbf{H}_{\mathrm{k}}^{\#} = \left(\vec{0}^T, -\vec{e}_k^T, \vec{0}^T, \vec{0}^T, \vec{0}^T, 0, 1 \right) \int_{\mathrm{t_{k-1}}}^{\mathrm{t_k}} \mathbf{\Phi}_{t,t_{k-1}} dt \cdot \mathbf{\Phi}_{t_{k-1},t_k} \qquad (13)$$

Where $\hat{\vec{\mathrm{L}}}_{\mathrm{k-1}}^{\mathrm{n}}$ is the lever arm at the previous time step and $\delta\hat{\vec{\mathrm{L}}}_{\mathrm{k}}^{\mathrm{n}}$ is the change in the lever arm in two consecutive time steps. The integral of the transition matrix factorization truly accounts for the dynamics during the time interval $[t_k, t_{k-1}]$.

This formulation is now extended by the measured carrier frequency error $\Delta\tilde{f}_{ca}$ multiplied by Δt which can be interpreted as a change of the LOS distance

$$\Delta y_k = \hat{y}_k - \tilde{y}_k + \Delta\tilde{f}_{ca,k}\lambda\Delta t \qquad (14)$$

The averaging effect of the carrier frequency discriminator is combined with an accurate formulation of the relative movement during time interval of the correlator. To distinguish between the original ADR algorithm and the derived version, the authors called it *virtual-ADR*. High accelerations and jerks are truly accounted for by numerically integrating the transition matrix containing the inertial measurements. In the following chapter the correlation time will be extended, which emphasizes the necessity of this formulation.

4. REDUCING NOISE

Extending the predetection integration time results in a decreased noise standard deviation of the measured frequency error. The influence on the noise reduction of the velocity estimation will be explained by theoretical estimations of the carrier frequency discriminator and will be verified by simulated data.

Following an expansion of the integration time of the discriminators from 20ms (2x10ms) up to 100ms (2x50ms) is carried out. Therefore not only the PIT is varied, also the estimation step of the Kalman filter has to be synchronized, due to the usage of the discriminator output values in the data fusion algorithm in a deeply coupled system. The aim of the extended signal integration time is a reduction of the noise level of the GPS-measurements.

In the simulation there is no GPS navigation data modulated upon the signal. That means that the influence of the algebraic sign of navigation data on the *I/Q*-samples, used in the discriminators, do not have to be taken into account explicitly. An estimation of the navigation bits allows an extended integration time even in case of bit transitions. Thus an expansion of the PIT can be realized and tested.

The carrier frequency discriminator uses a four-quadrant arctan-function. The processing is done by means of the dot- and cross-product, whereas the utilized sums of the inphase- and quadrature-components are divided into two time-sections. $I_{PS,1}$ and $Q_{PS,1}$ represent the accumulated values of the first time-section of the non shifted signal (prompt). On the other hand $I_{PS,2}$ and $Q_{PS,2}$ use the accumulated values of the second half of the PIT.

The working area of this carrier frequency discriminator depends on the reciprocal value of the PIT [8]. A higher PIT leads to a smaller pull in range. That means that the working area is restricted, which can cause problems especially in during high frequency errors caused by a low carrier frequency update rate. But a higher integration time also leads to reduction of the noise level of the discriminator output.

The variance of the normalized error signal of the carrier frequency discriminator is described according to the derivation in [1]

$$\sigma^2\{\Delta f\} = \frac{1}{(2\pi)^2 (N-1)^2 \frac{c}{n_0} T_{CO}^3} \left(1 + \frac{N-1}{\frac{2cT_{CO}}{n_0}} \right) \qquad (15)$$

A closer lock at equation (15) shows that in case of high SNR the last factor within the brackets is smaller than one and does not have a significant influence. On the other hand, at low SNR values, this term has a strong effect.

For high SNR the equation can be re-written with a constant factor C :

$$\sigma^2\{\Delta f\} = C\frac{1}{T_{CO}^3} \qquad (16)$$

Using two different coherent integration times T_{CO} one obtains:

$$\sigma^2\{\Delta f_{10}\} = C\frac{1}{(10ms)^3}, \quad \sigma^2\{\Delta f_{50}\} = C\frac{1}{(50ms)^3} \qquad (17)$$

The relevant factor between a predetection integration time of 10ms and 50ms of the standard deviation $\sigma\{\Delta f\}$ for high SNR is:

$$\left(\frac{1}{5}\right)^{\frac{3}{2}} \approx 0.089 \qquad (18)$$

For the influence on the accuracy of the velocity estimation the multiplication with T_{CO} has to be considered. The resulting theoretical noise reduction is

$$\left(\frac{1}{5}\right)^{\frac{3}{2}} \cdot 5 \approx 0.447\,. \qquad (19)$$

Comparing these theoretical values with the simulation results shown in figure 1 leads to the following standard deviation of the frequency errors:

$$\begin{aligned} T_{CO} &= 10ms \quad \rightarrow \quad \sigma\{\Delta f_{10}\} = 1.2584\text{Hz} \\ T_{CO} &= 50ms \quad \rightarrow \quad \sigma\{\Delta f_{50}\} = 0.1247\text{Hz} \end{aligned} \qquad (20)$$

For the influence on the accuracy of the velocity estimation the multiplication with T_{CO} has to be considered. The resulting experimental noise reduction is

$$\left(\frac{0.1247}{1.2584}\right) \cdot 5 \approx 0.495 \qquad (21)$$

This is a sufficient validation of the theoretically predicted noise performance improvement.

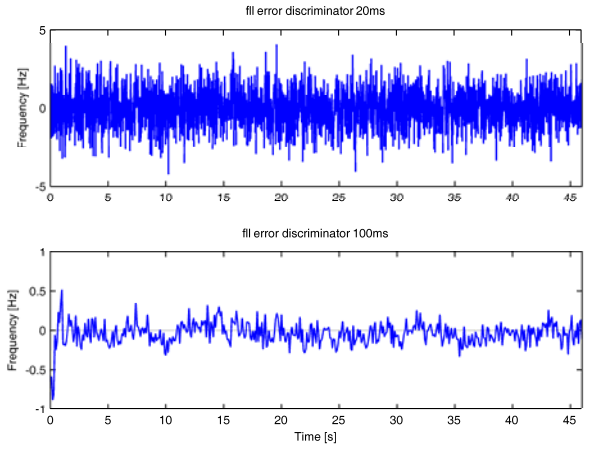

Fig. 1: Measured Carrier frequency error with different predetection integration time intervals (2x10ms and 2x50ms) during an unacc. flight

For low SNR the latter term of equation (15) will be relevant. The relative reduction of the velocity error standard deviation will be even more:

$$\left(\frac{1}{5}\right)^{\frac{4}{2}} \cdot 5 = 0.2 \qquad (22)$$

5. CARRIER REPLICA UPDATE

A deeply coupled system uses the estimated velocity $\hat{\vec{v}}$ and the estimated clock error drift $\delta\hat{t}_U$ of the Kalman filter solution to calculate the Doppler-afflicted carrier frequencies $\hat{f}_i$ by using the satellite geometry and velocity. Thus the NCOs can be adjusted directly by using the determined satellite-individual estimation-values. Because of this direct feedback there is no controller necessary at this place. Because of the fact that new sensor-measurement-values of the IMU are available every millisecond and are used in order to calculate a navigation solution in the SDA, each millisecond an updated state space estimation is received. It is immediately possible to use the high data rate of 1ms of an IMU instead of a carrier replica update rate of 20ms in the GPS-receiver. Figure 2 shows the structure of a deeply coupled system with an update rate of the carrier replicas of 1ms. It can be seen that the potential of an update rate of 1ms is used. To analyze the system behavior and the robustness of the system an output of the function h is realized every millisecond and processed in the software receiver. In real hardware systems there is of course a dependency of the IMU data rate and the used GPS-receiver-interface.

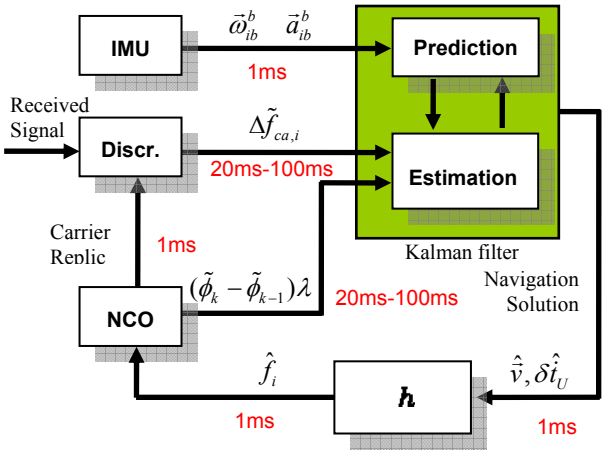

Fig. 2: Carrier replica update with 1ms

6. SIMULATION ENVIRONMENT

The aim of this research is the development of a deeply coupled system with the ability of a robust signal-tracking in extreme flight manoeuvres. Especially in cornering lateral accelerations occur. This leads to strong changes of the relative movement between a satellite and the receiver. In order to analyze the quality of the implemented tracking and navigation algorithms of the deeply coupled system in Embedded Matlab/Simulink, a flight scenario was created, that represents the trajectory of a fast moving and strongly accelerated object. Therefore the IMU sensor data over time and the corresponding received GPS-signals,

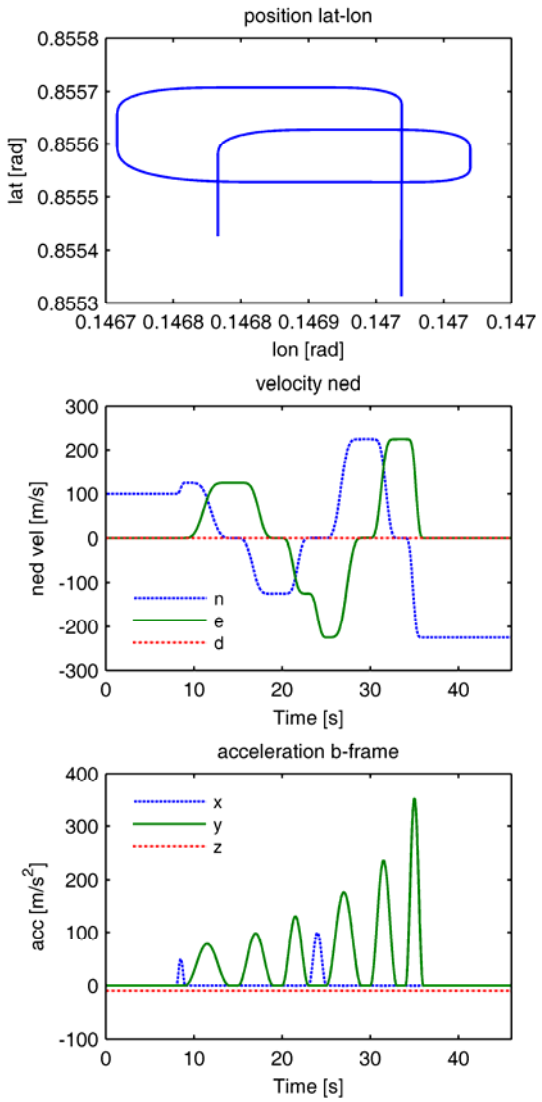

Fig. 3: Ground track, velocity in navigation frame and acceleration (up to 35g) in body-frame of the trajectory

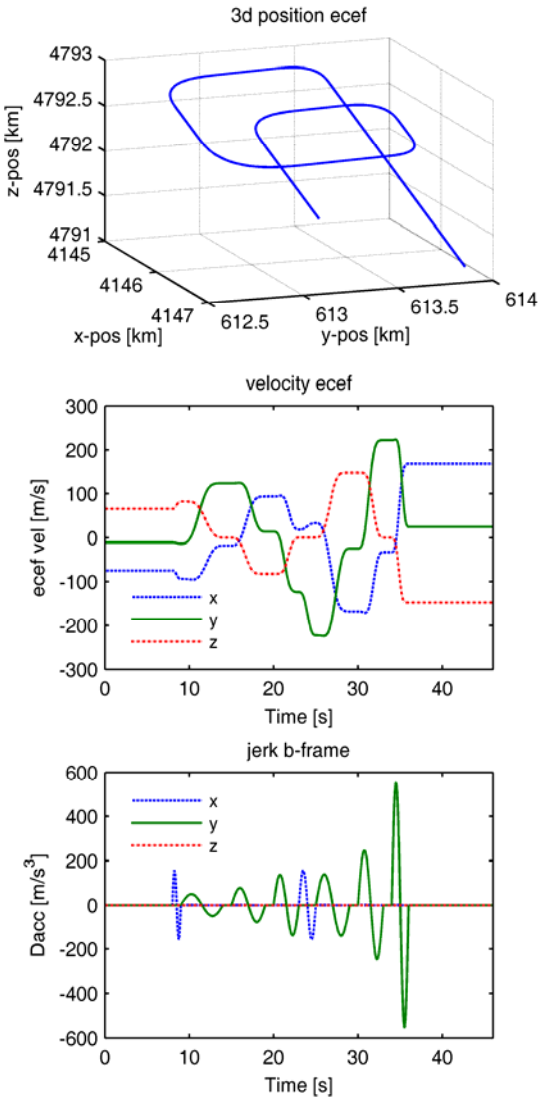

Fig. 4: 3D track, velocity in ecef frame and jerk (up to 500 m/s^3) in body-frame of the trajectory

which are Doppler-afflicted because of the relative movement of the satellite and the receiver, time shifted, damped and superposed by noise, are generated. The overlaid GPS-signals of different satellites are used in the user segment on the bases of intermediate frequencies, whereas the IMU data is processed in the strapdown algorithm (SDA) to calculate an absolute navigation solution. Following the characteristics of a tactical grade IMU, the ideal sensor data is overlaid by white noise, and sensor biases are added. The created trajectory comprises several situations with extremely high acceleration and jerk values. The flight starts straight on in a northbound direction with an initial velocity of 100m/s and an initial attitude of the roll-, pitch- and yaw-angle of 0 degrees. The further progression of the flight shows six 90 degree spiralings with varying durations of these individual maneuvers. In between the object is accelerated up to a velocity of 225m/s. All in all, the entire scenario lasts 46 seconds. During that time the SNR of all received satellite signals remains constant at a high level. Figure 3 and figure 4 visualize the characteristics of the used trajectory. It can be seen that the values of the accelerations given the body-frame increase in every spiraling over time, due to the rising velocity and the alternation of the duration of the single flight maneuver. At second 35 a maximum lateral/transverse acceleration of 35g and a jerk of up to 500 m/s^3 is reached. Previous simulations showed that standard tracking loops loose the track of the satellite signals in such extreme situations. As a consequence there is no aiding information of the GPS available, which results in a divergence of the navigation solution.

The simulation environment provides a full 6-degrees of freedom (DOF) simulation of satellite orbits and receiver trajectory. In a first step, the receiver trajectory is generated according to a given maneuver schedule. The starting point, starting velocity and attitude can be chosen arbitrarily in WGS-84 coordinates. From the initial setup the trajectory generation follows given changes in velocity, angle or height. In addition, attitude variations can be simulated but this is not used in the presented scenario. To examine tracking loop characteristics in the presence of dynamic stress, a smooth change in acceleration is

essential. Therefore the jerk is not modeled by a step function but by a sinusoid during trajectory dynamics. The resulting trajectory is used as an ideal reference and is the basis in the 6-DOF simulation of satellite receiver geometry.

Based on the simulated satellite receiver geometry, the digital sampled IF signal is generated. This includes the signal time delay and implicitly the Doppler effect. The signal is filtered by a band-pass filter with a bandwidth of 4 MHz. The sampling frequency is 38.192 MHz and the intermediate frequency is set to 9.548 MHz.

After band-pass filtering, an automatic gain control is applied to optimally cover the range of the following A/D converter. The resulting signal is sampled in 2 bits and is finally processed in a software receiver consisting of different channels and a navigation process as shown in figure 5.

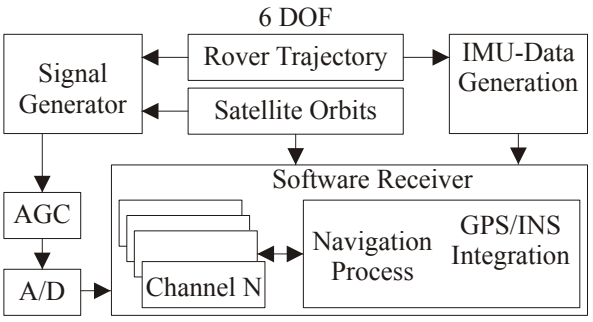

Fig. 5: Simulation Environment

The simulation platform for the used deeply coupled system is Embedded Matlab/Simulink. In this environment several interacting function-blocks are implemented in order to allocate different tasks. All in all the simulation model is divided into four blocks, connected to broadcast the appropriate information. Besides a function-block *Tracking* there also exist the functions *Satorbits*, *Position*, and mapping function *h*. *Tracking* comprises the basic GPS-signal-tracking with components like the numerically controlled oscillators (NCO), discriminator functions and the corresponding controllers. This allows evaluating the Doppler-afflicted carrier frequencies and the shift in phase for every single satellite, based on a simulated GPS-signal. In addition an estimation of the quality - that means the variance - of the calculated pseudorange and delta-range is implemented. Dependent on the structure of the integrated system, different function-block outputs are possible. In a deeply coupled system the output values of the discriminators are also supplementary used in the block *Position*, which comprises the data fusion algorithms and the strapdown algorithm (SDA) in order to estimate a navigation solution. In case of the usage of *virtual-ADR* measurements the appropriate function in the Position block is utilized in the filter step of the closed loop error state space Kalman filter (KF), instead of the delta-range measurements. The filter step of the KF is synchronized with the availability of the GPS-measurements of the *Tracking* block. Because of the nonlinear mathematical models a linearization has to be done in order to use the standard Kalman filter model. As a result the error terms of the state space vector are estimated. Consequently the absolute navigation solution of the strapdown algorithm - based on the sensor values of the inertial measure unit (IMU) - is corrected. In the deeply coupled system the function-block *h* provides the satellite-individual error in distance and the Doppler-afflicted carrier frequencies, based on the estimated position and velocity solution of the KF. The estimated clock error and drift are also considered. Thus a feedback to the *Tracking* block is realized and the control circuit is closed. The fourth block *Satorbits* calculates the position and the velocity of single satellites over time by using orbit data. These values are required to calculate the distance between the receiver and the satellites and also the individual relative velocity. In the simulation a fixed step size of 1ms is used, equivalent to the data rate of the simulated IMU.

7. SIMULATION RESULTS

In this section a comparative overview over the simulation results of various implemented system models with different configurations is shown. The description of the results is generally divided into deeply coupled systems with an update rate of the carrier replica of 20ms and 1ms. To show the impact of various system configurations on the navigation result, two different predetection integration times (PIT) of the discriminators and two different implementations of the Kalman filter estimation steps are combined. On the one hand PITs of 2x10ms and 2x50ms are used, in combination with the measurement value processing of the GPS-delta-range or *virtual-ADR*. The listed figures below show the absolute error. At each time step the Euclidean distance between estimated and the true trajectory is calculated.
In figure 6 the absolute velocity error in coordinates of the ecef-frame is illustrated. In deeply coupled systems using discriminators with a PIT of 2x50ms an increasing error over time can be recognized. These implementations are not able to track extreme dynamics of the trajectory exactly enough in case of an update rate of the carrier replicas of 20ms. This results in a divergence of the calculated navigation solution. Because of the smaller operating range of the carrier frequency discriminator due to the increased PIT of 2x50ms instead of 2x10ms, a loss of lock can occur. This means that the correct operating range of the frequency-accurate adaption is left. In order to avoid this behavior and to stay within the pull-in-range of the discriminator an exacter - that means faster - update/feedback of the carrier replicas is necessary. In the following section the results of this higher update rate will be shown. The use of discriminators with an increased PIT, in order to calculate GPS measurement values with a low noise level, is not a reasonable step for the described scenario and the chosen update rate of the carrier replicas. However systems with a PIT of 20ms deliver - analog to figure 6 - convergent estimations of the system states. But especially in the

case of processing delta-ranges - also called Doppler-measurements - strong influences of the trajectory dynamics on the estimated solution can be recognized. These influences correspond with the appearance of high accelerations during the flight. A better result is achieved by using the virtual accumulated delta range (*virtual-ADR*).

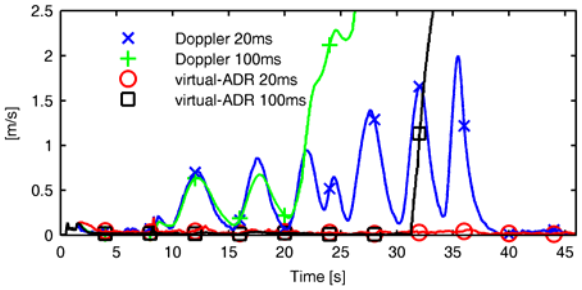

Fig. 6: Velocity error with 20ms carrier frequency update time

The simulation results in figure 7 with a carrier replica update of 1ms consistently show convergent navigation solutions. That means that within the simulation time the absolute velocity error stays below a certain threshold. However there exist differences concerning the quality of the estimations. Deeply coupled system implementations with a PIT of the discriminators of 2x10ms deliver a noticeable higher noise level. On the other hand the use of discriminators with a higher PIT - in this case 2x50ms - leads to a reduction of the noise level of the discriminator outputs. These discriminator outputs are processed in the estimation step of the Kalman filter, in order to support the navigation solution. As a consequence the noise level of the appropriate state space solution is also reduced. In figure 7 this characteristic is depicted in the form of smoother error patterns for the two models "*Doppler 100ms*" and "*Virtual-ADR 100ms*" in comparison to the models with a PIT of 2x10ms.

Overall, the use of a higher update rate of the carrier replica signals in the deeply coupled system leads to a higher accuracy in tracking. As a result the Doppler-afflicted carrier frequency is adapted in a faster way and shows a smaller frequency error. Such a system allows tracking satellites even in the occurrence of extreme trajectory dynamics. Hence a continuous support in the KF estimation step is possible, and a divergence of the short-time accurate inertial navigation solution can be prevented. Especially the processing of *virtual-ADR* measurements generates very low velocity errors over time. The navigation solution is not strongly influenced by high dynamics during the simulated maneuvers. In the end a robust, reliable and long term accurate result is obtained. The results show an error value under the threshold of 5cm/s and also a smooth signal characteristic over time. In addition the absolute position error of the estimation also is not strongly influenced by high dynamics. The position estimation shows a smooth error as well, but the position solution will be offset by uncorrected ionosphere and troposphere errors.

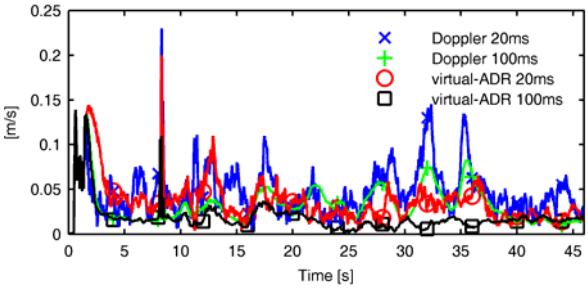

Fig. 7: Velocity error with 1ms carrier frequency update time

CONCLUSIONS

By reformulating the velocity measurement step of a non-coherent deeply coupled GPS/INS system it was adapted to correctly account for the averaged measurement values of the carrier frequency discriminator. This results in a decreased velocity error especially in high dynamic environments. With this method the predetection integration time in the baseband processor may be extended without suffering from dynamic stress in the measurement step.

REFERENCES

[1] Misra, P., and Enge, P., Global Positioning System - Signals, Measurements, and Performance. 2. Edition. Lincoln, Massachusetts: Ganga-Jamuna Press, 2006, CD Enge, P.: White Noise Analysis of the Frequency Lock Loop, 2004

[2] Farrel J.L. GPS/INS-Streamlined. In *NAVIGATION Journal of the Institute of Navigation*, Vol. 49 No. 4, 2002

[3] Wendel J. et. Al. Time-Differenced Carrier Phase Measurements for Tightly Coupled GPS/INS Integration. In *Proceedings IEEE PLANS,* April 2006

[4] Groves, P.D. Mather, C.J. and Macaulay, A.A. Demonstration of Non-coherent Deep INS/GPS Integration for Optimised Signal-to-noise Performance. In *Proceedings ION GNSS,* September 2007

[5] Groves, P.D. and Long, D.C. Adaptive tightly-coupled, a low cost alternative anti-jam INS/GPS integration technique. In *Proceedings ION NTM*, January 2003

[6] Soloviev A., Gunawardena, S., and, van Graas, F. Deeply Integrated GPS/Low-Cost IMU for Low CNR Signal Processing: Concept Description and In-Flight Demonstration. In *NAVIGATION Journal of the Institut*e of Navigation, Vol. 55 No. 1, 2008

[7] Landis D. et. Al. A Deep Integration Estimator for Urban Ground Navigation. In Proceedings IEEE PLANS April 2006

[8] Kaplan, E.: Understanding GPS Principles and Applications. Artech House, 1996.